[Article ID] 1003- 6326(2001) 03- 0350- 03

XU Yan-hui(徐艳辉), CHEN Chang-pin(陈长聘), LI Shou-quan(李寿权), YING Tiao(应 宽), WANG Qrdong(王启东)
(Department of Materials Science and Engineering, Zhejiang University, Hangzhou 310027, P. R. China)

[Abstract] The rapid development of electric vehicles demands the development of high performance nickel metal hydride battery that is able to endure high temperature. The discharge properties of $Ti_{0.7}Zr_{0.5}V_{0.2}Mn_{1.8-x}Ni_x$ (x=0.4, 0.8, 1.1, 1.4, 1.7) hydrogen storage alloys was investigated and its phase composition was analyzed using X-ray diffraction. The results show that the cycling life was improved as the content of nickel increases. When x=0.4, 0.8, 1.1 and 1.4, the main phase is $MgZn_2$ type C14 Laves phase and the second one is cubic TiNi phase. When x=1.7, the Laves phase structure disappears. EDAS analysis shows that the increase of nickel content is effective in suppressing the dissolution of vanadium component in alloys.

[Key words] hydrogen storage electrode alloys; high temperature electrochemical performance; phase composition [CLC number] TG 139 [Document code] A

1 INTRODUCTION

The rapid development of electric vehicles is inevitable because of less environmental pollution. Now, one of R&D directions is focused on the EV in USA, Japan, Canada etc to satisfy the requirement of the rapid development of transportation, energy and environment. Fuel cell^[1, 2], Li⁺ secondary battery^[3] and NrMH battery^[4, 5] are the promising candidate driving power. Pb-acid secondary battery has been used in electric bike and electric scooter. Pb-acid battery would be replaced by other batteries, firstly by NiMH battery, because of its low energy density (only 30 Wh/kg). When electric vehicle accelerates, the time output power is large and the output current is also high. Therefore the temperature inside battery is higher, which indicates that the metal hydride electrode must have good high-temperature properties. Based on the discussion above mentioned, in this parper the properties of $Ti_{0.7}ZR_{0.5}V_{0.2}Mn_{1.8-x}Ni_x(x=$ 0.4, 0.8, 1.1, 1.4 and 1.7) hydrogen storage alloys at 323 K and 353 K are investigated, including activation behavior, discharge capacity and phase composition etc.

2 EXPERIMENTAL

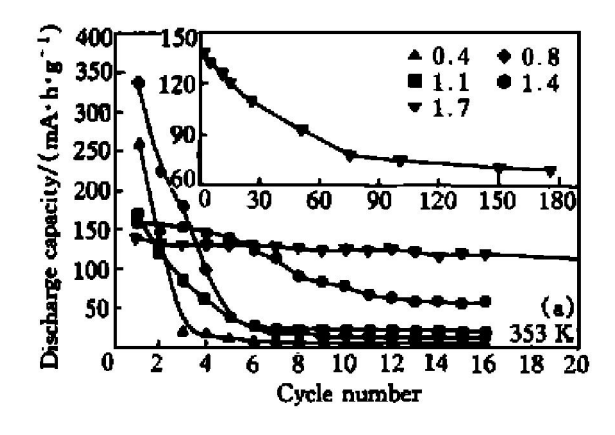
The purity of all used original materials is higher than 99. 5%. The ingot was prepared by highfrequency induction melting and then mechanically

pulverized to powder for electrochemical measurement and X-ray diffraction analysis. The electrode preparation method is the same as that listed in Ref. [6]: the mixture of alloy powder and nickel powder (mass ratio is 1:2) was pressed at 1.5 MPa to a round disk electrode with a diameter of 10 mm and thickness of about 1 mm; the content of alloy powder is about 200 mg. The charging discharging cycle current is 25 mA/g. The reference electrode is Hg/HgO/6 mol/L KOH and the positive electrode is Ni(OH) 2/NiOOH electrode using 6 mol/ L KOH electrolyte. Environment temperatures were set up at 323 K and 353 K, respectively. The end point of discharge was set at - 0.6 V. The charging discharging cycle was measured using DC-5 Battery Test Instrument. The Philips X' pert diffractometer was used for phase analysis; the power is $40 \text{ kV} \times 20 \text{ mA}$ and the scanning rate is 0.04(°)/s. The energy dispersive analysis was measured at PV9900-Philips energy analyzer to analyze the element content change before and after electrochemical cycling; the duration time is 100 s.

3 RESULTS AND DISCUSSION

The cycling life of $Ti_{0.7}Zr_{0.5}V_{0.2}Mn_{1.8-x}Ni_x(x = 0.4, 0.8, 1.1, 1.4, 1.7)$ hydrogen storage alloys at 323 K and 353 K is shown in Fig. 1. At 353 K, all used alloys reach the maximum discharge capacities at the first cycle without any action. At 323 K, the action is not needed for x = 0.4, and the action number

① [Foundation item] Project (715-004-0060) supported by the National Advanced Materials Committee of China [Received date] 2000-07-12; [Accepted date] 2000-09-22



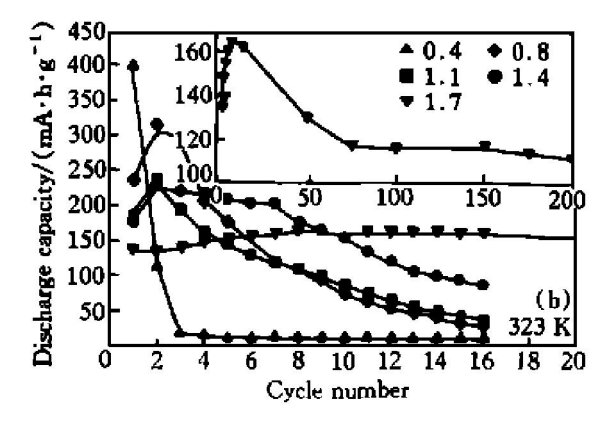


Fig. 1 Cycling life of $Ti_{0.7}Zr_{0.5}V_{0.2}Mn_{1.8-x}Ni_x$ alloys (Charge discharge current density: 25 mA/g)

increases as the content of nickel in alloys increases.

At 353 K, when the x changes from 0. 4 to 0. 8 the maximum discharge capacity increases, while when the x value changes from 0. 8 to 1. 7 it decreases. When x=0. 8, the maximum capacity is 336 mAh/g, the corresponding hydride is $Ti_{0.7}Zr_{0.5}V_{0.2}Mn_{1.0}Ni_{0.8}H_{2.40}$. At 323 K, the maximum discharge capacity decreases with the content of nickel in alloys. It is 399. 1 mAh/g for x=0. 4, the corresponding hydride is $Ti_{0.7}Zr_{0.5}V_{0.2}Mn_{1.4}Ni_{0.4}H_{2.76}$. When the environment temperature increases from 323 K to 353 K, the discharge capacity of all the used alloys decreases except $Ti_{0.7}Zr_{0.5}V_{0.2}Mn_{1.0}Ni_{0.8}$ alloy.

From Fig. 1, it can be seen also that after about 10 cycles, the discharge capacity increases with the content of nickel in alloys. This indicates that the increase of the content of nickel is effective for improving the cycling stability. The increase of environmental temperature from 323 K to 353 K worsens the cycling stability, for example, for x=0. 8, after about 9 cycles the discharge capacity at 323 K decreases to 100 mAh/g, while at 353 K only 4 cycles. Through 16 charging discharging cycles, the discharge capacity of all alloys decreases to be smaller than 100 mAh/g except the Ti_{0.7} Zr_{0.5} V_{0.2} M n_{0.1} Ni_{1.7}, regardless of the temperatures.

The powder X-ray diffraction patterns are shown in Fig. 2, and the cell parameters were listed in Table 1. The lattice parameters were calculated by the following equation:

$$\frac{1}{d^2} = \frac{4}{3} \left(\frac{h^2 + hk + k^2}{a^2} \right) + \frac{L^2}{c^2}$$
 (1)

where d represents the distance between faces, hkl are the corresponding lattice indexes, a and c are the corresponding lattice constants for C14 Laves phase. In this paper, the diffraction values of (103) and (112) faces were used to calculate a and c.

Eliiot et al^[7] studied the relation between the Average Number of Outer Electrons (ANOE) and phase structure and found the following results: for AB₂ type compounds, when A-side atom is Ti or Zr,

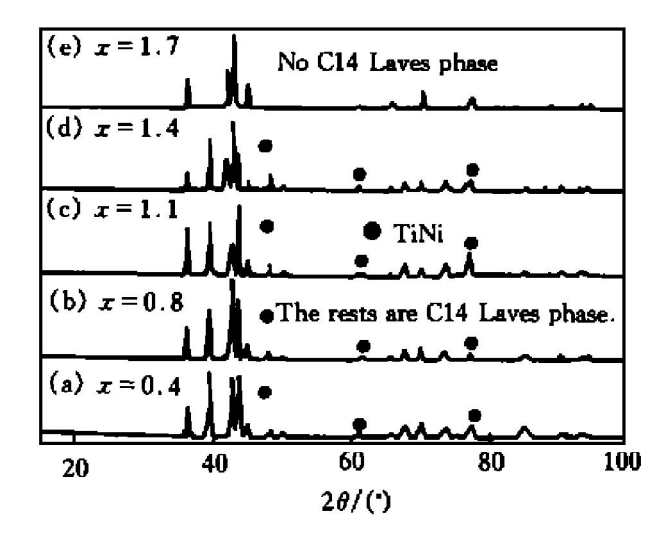


Fig. 2 XRD patterns of $Ti_{0.7}Zr_{0.5}V_{0.2}Mn_{1.8-x}Ni_x$ alloys

B-side atom is V, Cr, Mn, Fe, Co, Cu or Zn, when ANOE < 5.4, no Laves phase appears for Ti and C15 Laves phase appears for Zr; when 5.4< ANOE< 7.0 the C14 Laves phase appears; when ANOE> 7.0 the C15 Laves phase appears. The X-ray analysis shows that, when the x value changes from 0.4 to 1.4, the main phase is C14 Laves phase with MgZn₂ type structure and the second phase is cubic TiNi phase. When the x is 1. 7, the main phase is C15 Laves phase and the TiNi phase was also found. From Table 1 it can be seen that the lattice parameter a firstly increases then decreases, the parameter c decreases continuously, and the cell volume firstly increases then decreases with the x value. When the ANOE> 7. 0 the C14 Laves phase disappears and C15 phase appears, which is in agreement with the conclusion reported by Eliiot et al.

EDAS was used to analyze the element composition change at alloy surface before electrochemical cycle and after 20 cycles. The following phenomena were found: 1) for all as-cast alloy powders, the contents of Mn and V element are higher than the average contents in bulk, on the contrary, the content of Ti

Table 1 X-ray diffraction parameters of $Ti_{0.7}Zr_{0.5}V_{0.2}Mn_{1.8-x}Ni_x$

(x = 0.4, 0.8, 1.1, 1.4, 1.7) alloys

Alloy	a/ Å	c/ Å	V/ Å	c/a	Main phase	Second phase	ANOE
$Ti_{0.7}Zr_{0.5}V_{0.2}Mn_{1.4}Ni_{0.4}$	4. 918 1	8. 059 7	168. 828	1. 638 8	C14	TiNi	6. 13
$Ti_{0.7}Zr_{0.5}V_{0.2}Mn_{1.0}Ni_{0.8}$	4. 932 2	8. 034 8	169. 273	1.6290	C14	TiNi	6. 50
$Ti_{0.7}Zr_{0.5}V_{0.2}Mn_{0.7}Ni_{1.1}$	4. 924 7	8.0172	168.389	1.6280	C14	TiNi	6. 78
$Ti_{0.7}Zr_{0.5}V_{0.2}Mn_{0.4}Ni_{1.4}$	4.9195	8.0102	167.887	1. 628 3	C14	TiNi	7. 06
$Ti_{0.7}Zr_{0.5}V_{0.2}Mn_{0.1}Ni_{1.7}$	No Laves phase						

and Zr is lower than the average composition, and the difference between surface content and bulk content for Zr and Mn elements is relatively large, 2) compared with the as-cast alloy powders, after 20 cycles the change tendency of element content at alloy surface is listed in Table 2, the content of V element at surface decreases and the decrease range becomes small as the content of nickel in alloy increases, 3) after 20 cycles, the contents of Ti and Zr at surface decrease for x = 0.4 and increase for x > 0.4.

Table 2 Change tendency of element contents at surface after 20 electrochemical cycles

A 11	Change of each element						
Alloy	Тi	Zr	\mathbf{V}	Mn	Ni		
$Ti_{0.7}Zr_{0.5}V_{0.2}Mn_{1.4}Ni_{0.4}$	*	↓	↓	1	1		
$Ti_{0.7}Zr_{0.5}V_{0.2}Mn_{1.0}Ni_{0.8}$	↑ * *	1	↓	1			
$Ti_{0.7}Zr_{0.5}V_{0.2}Mn_{0.7}Ni_{1.1}$	1	1	1	1	1		
$Ti_{0.7}Zr_{0.5}V_{0.2}Mn_{0.4}Ni_{1.4}$	1	1	ļ	ţ	ļ		

Indicates the increase of this element content after 20 cyclings.

EDAS analysis shows the easy resolution of the V element at alloy surface in Laves phase alloy. It is believed that the reasons why the cycling life of alloys is poor and why the cycling life is improved by increase of the content of nickel element are as follows.

- 1) The V element in Laves phase alloy is easy to resolve in strong alkaline solutions. The destruction of Laves phase structure induces the decrease of discharge capacity.
- 2) The formation of the oxides^[8] at the alloy surface that can decrease the conductivity causes the decrease of discharge capacity.
- 3) The increase of nickel content in alloy can efficiently decrease the resolution of V element. Besides, the increase of nickel content at alloy surface promotes the improvement of the conductivity, and the increase in the resistance to corrosion. As a re-

sult, the discharge capacity is improved.

From the experiment results it can be seen that when the Mn content is 1. 4% (mole fraction), the discharge capacity at 323 K is 399. 1 mAh/g, but its cycling stability is very poor. Nickel replacing manganese remarkably promotes the increase of the cycling stability. For example, when x value is 1. 7, after 16 cycles the decay in discharge capacity is negative. For $\text{Ti}_{0.7}\text{Zr}_{0.5}\text{V}_{0.2}\text{Mn}_{1.8-x}\,\text{Ni}_x$ (x = 0. 4, 0. 8, 1. 1, 1. 4 and 1. 7) serial alloys, based on keeping the Laves phase structure and its discharge capacity, the synthetic electrochemical properties of $\text{Ti}_{0.7}\text{Zr}_{0.5}\text{V}_{0.2}$ Mn_{0.4}Ni_{1.4} alloy is relatively good. But the cycling stability cannot satisfy the practical application requirement and needs to be further improved.

[REFERENCES]

- [1] Morita K, Iwai N, Notoya O. Advanced clean energy vehicle project in Japan [A]. 16th Int Elect Vehicle Symp Proceed [C]. Beijing China, 1999.
- [2] MAO Z Q, YAN J, LIU L Y. The history, current situation and prospect of fuel cell in China [A]. 16th Int Elect Vehicle Symp Proceed [C]. Beijing China, 1999.
- [3] Okada M, Yasuda H, Yamachi M, et al. Porous polymer electrolyte Li ion battery with superior performance [A]. 16th Int Elect Vehicle Symp Proceed [C]. Beijing China, 1999.
- [4] WU B R, ZHAN F. Study on prismatic sealed Ni/MH battery for Evs [A]. 16th Int Elect Vehicle Symp Proceed [C]. Beijing China, 1999.
- [5] Kohler U, Ullrich M. High power nickel-metal hydride batteries [A]. 16th Int Elect Vehicle Symp Proceed [C]. Beijing China, 1999.
- [6] CHEN Li xin. Effects of Mg doping on electrochemical properties of Ml(NiCoMnTi)₅ hydrogen storage electrode alloy [J]. The Chinese Journal of Nonferrous Metals, (in Chinese), 1999, 9(1): 61-64.
- [7] Eliiot R P, Rostoker W. The occurrence of Laves type phases among transition metals [J]. Trans Am Soc Met, 1958, 50: 617.
- [8] Jung Jae Han, Lee Ham Ho, Kim Dong Myung, et al. Degradation behavior of Cur coated Tr Zr V-Mm Ni metal hydride electrodes [J]. J Alloys Comp, 1998, 266: 266 – 270.

(Edited by PENG Chao qun)

^{* *} Represents the decrease of this element content after 20 cyclings.